Multi-proxy assessment of surface sediments using APPI-P FTICR-MS reveals a complex biogeochemical record along a salinity gradient in the Pearl River estuary and coastal South China Sea

Jagoš R. Radović,[1‡*] Wei Xie,[2,3*] Renzo C. Silva,[1] Thomas B.P. Oldenburg,[1] Stephen R. Larter,[1] Chuanlun Zhang[4,5,6*]

[1]Department of Geoscience, University of Calgary, T2N 1N4 Calgary, Alberta, Canada

[2]School of Marine Sciences, Sun Yat-sen University, Zhuhai, 519082, China

[3]Southern Marine Science and Engineering Guangdong Laboratory (Zhuhai), Zhuhai, 519082, China

[4]Shenzhen Key Laboratory of Marine Archaea Geo-Omics, Southern University of Science and Technology, Shenzhen, China

[5]Southern Marine Science and Engineering Guangdong Laboratory (Guangzhou), Shenzhen 518055, China

[6]Shanghai Sheshan National Geophysical Observatory, Shanghai 200062, China

The paper is a non-peer reviewed preprint submitted to EarthArXiv

Multi-proxy assessment of surface sediments using APPI-P FTICR-MS reveals a complex biogeochemical record along a salinity gradient in the Pearl River estuary and coastal South China Sea

Jagoš R. Radović,[1‡*] Wei Xie,[2,3*] Renzo C. Silva,[1] Thomas B.P. Oldenburg,[1] Stephen R. Larter,[1] Chuanlun Zhang[4,5,6*]

[1]Department of Geoscience, University of Calgary, T2N 1N4 Calgary, Alberta, Canada

[2]School of Marine Sciences, Sun Yat-sen University, Zhuhai, 519082, China

[3]Southern Marine Science and Engineering Guangdong Laboratory (Zhuhai), Zhuhai, 519082, China

[4]Shenzhen Key Laboratory of Marine Archaea Geo-Omics, Southern University of Science and Technology, Shenzhen, China

[5]Southern Marine Science and Engineering Guangdong Laboratory (Guangzhou), Shenzhen 518055, China

[6]Shanghai Sheshan National Geophysical Observatory, Shanghai 200062, China

[‡]Submitting author: Jagos.Radovic@ucalgary.ca

[*]Corresponding authors: Jagos.Radovic@ucalgary.ca; xiewei9@mail.sysu.edu.cn; zhangcl@sustech.edu.cn

TOC/Abstract Art

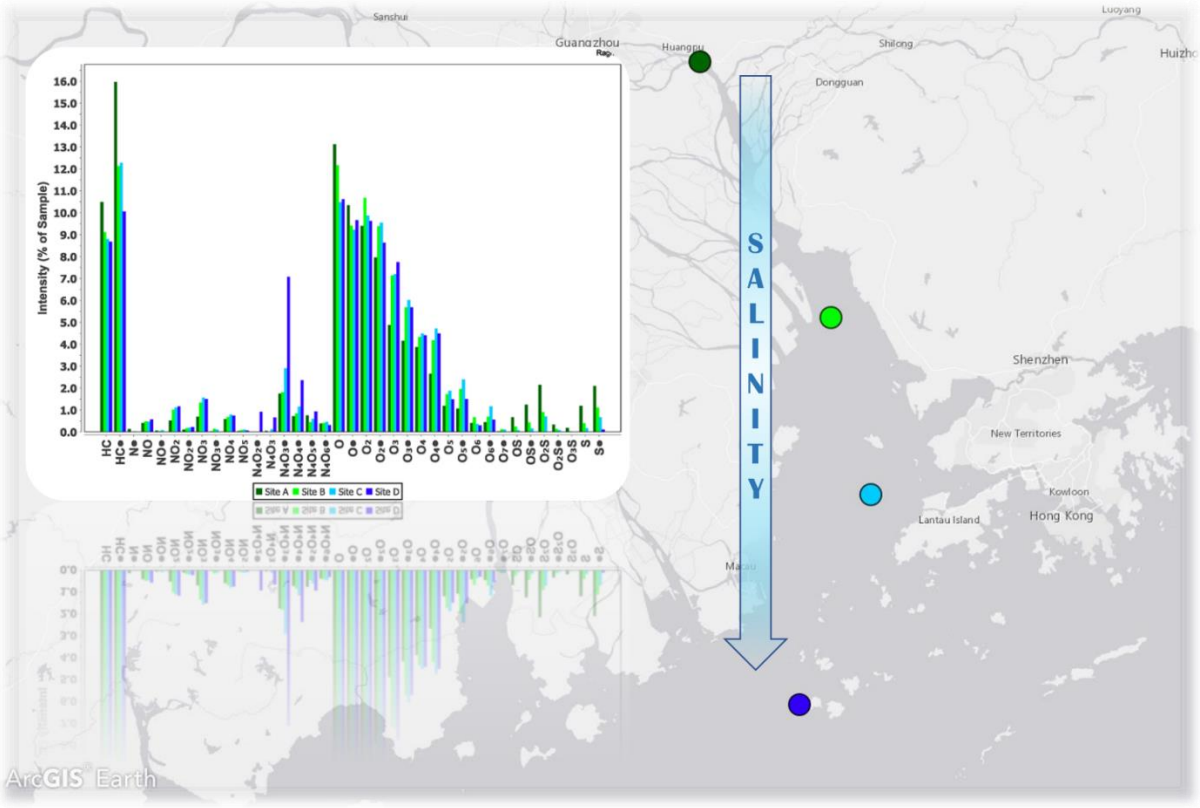

Abstract

The Pearl River drains the second largest watershed in China, funnelling large amounts of freshwater and organic matter into the northern part of the South China Sea through an estuary characterized by pronounced biogeochemical gradients. In this study we analyzed organic extracts of surface sediments collected along land-sea transect that captures a transition from freshwater environment at the site of the Pearl River discharge, to marine settings at the most distal sampling point in the coastal South China Sea. Samples were analyzed using Fourier transform ion cyclotron mass spectrometry (FTICR-MS), to assess the molecular composition of the organic species present in the sediment and understand the

sources and diagenesis of deposited organic matter. Results show a complex mixture of molecular markers, many of which can be used as proxies to distinguish between the freshwater and saline settings. For example, geochemical signal at the freshwater site is notably characterized by species belonging to hydrocarbon and sulphur-containing compound classes – these are likely markers of terrestrial, natural and/or anthropogenic organic matter inputs. On the other hand, samples from the coastal marine site bear a unique signature of putative tetrapyrrole species, molecular indicators of phytoplankton phaeopigments. Notably, some unusual and or novel species, such as sterenes and alkanones were putatively identified. These and other biomarkers species that can be detect using our single injection method provide convenient multiple proxies necessary for interpreting dynamic changes from land to the ocean, which have even been complicated by anthropogenic activities.

Keywords: Pearl River estuary, South China Sea, organic matter, sediment, biogeochemistry, molecular markers, FTICR-MS

Synopsis: Molecular markers in surface sediment reflect a shift in the nature of organic matter along the land-sea transect in the Pearl River estuary and coastal South China Sea.

1. Introduction

Estuaries are unique biogeochemical interfaces between terrestrial and marine environments. River discharges introduce natural and anthropogenic organic matter from the continent and create salinity and other physico-chemical gradients along the land-sea transect. In turn, these variable ecosystem conditions within estuaries create a dynamic structure of (micro)organisms and their communities.[1, 2] Ultimately all these complex processes and interactions end up being recorded and preserved in the geochemical composition of bottom sediments within estuaries.

Therefore, a better assessment of geochemical signals in estuarine organic matter deposition can afford novel insights into the sources and fate of organic carbon, on a global scale. On the other hand, molecular level assessment of sedimentary organic matter is a major analytical challenge, due to its chemical complexity and the presence of high molecular weight, and/or heteroatom (nitrogen, oxygen, sulphur) bearing species, such as carbohydrates, lignocellulose, pigments, lipids, and many other, still uncharacterized compounds. Therefore, analyses of molecular markers in sediments typically involve specific, targeted protocols, often including laborious fractionation steps, and use of different instruments, all in an attempt to improve sensitivity and resolution of targeted geochemical proxies. Only recently, developments of single-run methods that allowed investigators to simultaneously monitor multiple proxies of interest have emerged; notably, these novel methods use Fourier transform ion cyclotron resonance mass spectrometry (FTICR-MS) leveraging the capability of this analytical platform to screen for thousands of compounds, with a very high resolution over a broad analytical window of polarity and molecular weights.[3-9] While FTICR-MS approaches may lack the sensitivity and separation specificity of liquid chromatography-based approaches, they have an advantage of

simplified sample preparation, and the screening capability that can discover novel geochemical proxies and pathways.[6, 7]

With a length of ~2,400 kilometers, the Pearl River (PR) is the second largest river in China. It is located in the Guangdong Province and discharges into northern portion of the South China Sea (SCS). This region is characterized by subtropical climate, with high temperature and abundant, monsoon rainfalls, contributing to seasonally variable PR discharge into estuary, which on annual basis amounts to 54×10^6 tons of sediment.[10] Sources of organic matter transported by PR are heterogenous, and integrate influences of soil erosion in the upstream sections, contributions from lush subtropical vegetation in the mid-stream portion, and finally significant anthropogenic inputs from the downstream PR delta region, that houses 20 million people and hosts a burgeoning industrial sector. In addition to complex sources, processes of sediment remobilization and degradation further complicate biogeochemical assessments.[11, 12]

In this context, we used our recently developed FTICR-MS methodology[6, 7] to assess molecular composition of surface sediments collected along a transect in the Pearl River estuary and into coastal SCS. The objectives of the study were to relate molecular composition of surface sediments with a shift from freshwater to marine environment and derive new knowledge on the complex biogeochemistry of this estuarine system.

2. Materials and Methods

2.1. Sampling

Sediment samples were collected from the Pearl River estuary and coastal SCS (Guangdong, China) in January, February, April, and May of 2013, from surface sediment (0-5 cm depth) at

sites A, B, C and D, along a gradient of salinity and other physico-chemical parameters (Table S1), Fig. 1. The sampling transect line from site A to site D is approximately 125 kilometers long.

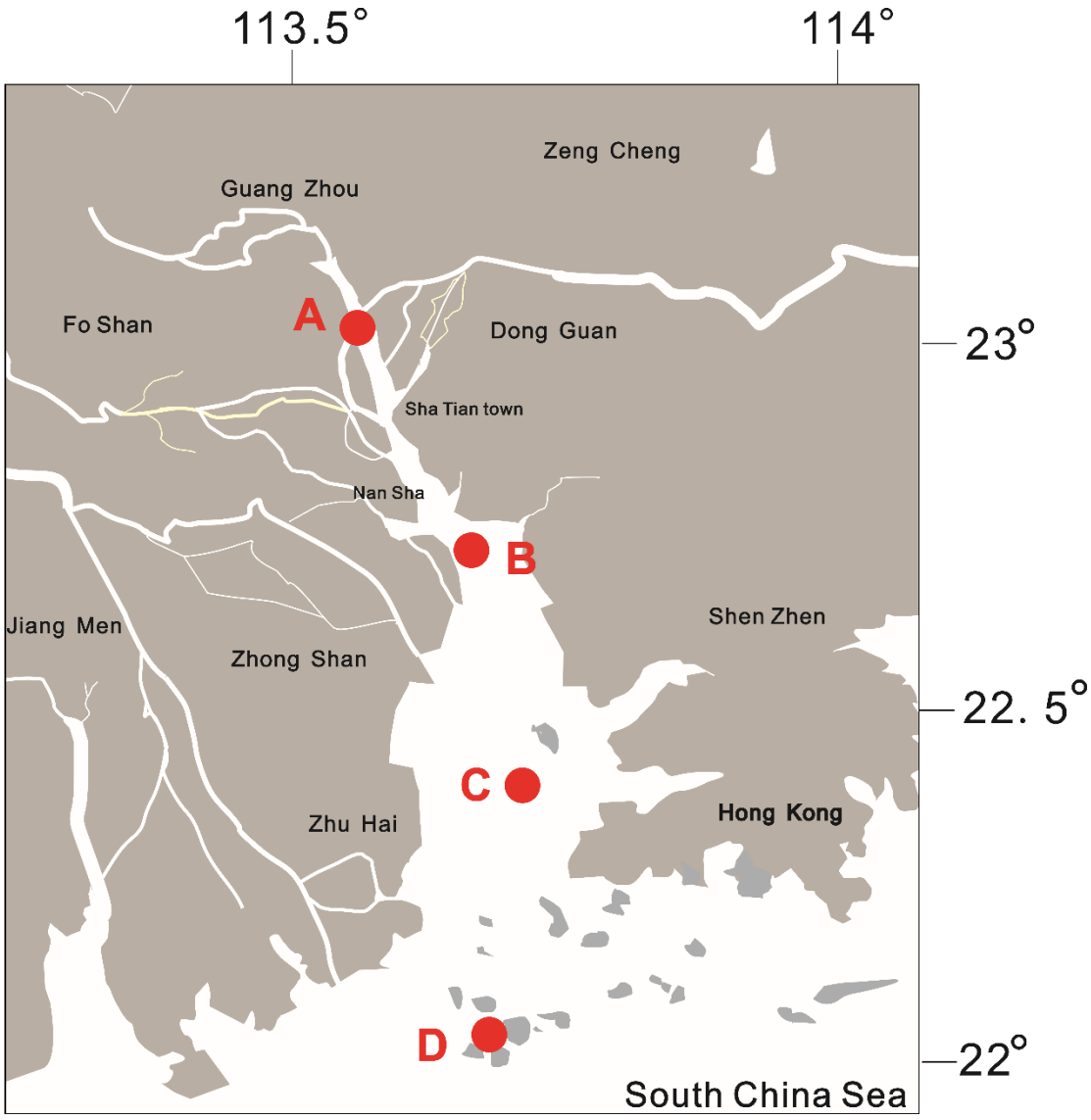

Figure 1. Map of the Pearl River estuary and coastal South China Sea showing sampling sites where surface sediments were collected.

Sediment samples were collected with a portable grab, transferred to sterilized centrifuge tubes (NEST, 50 ml), and immediately frozen and stored at -20°C until they were further processed. The salinity and pH of surface sediments were measured in situ by a conductivity

meter (SG3, Mettler-Toledo Instruments Co., Shanghai) and a pH analyzer (S20, Mettler–Toledo Instruments Co., Shanghai), respectively. Detailed sampling information is provided in the Table S1.

2.2. Sample Extraction

Freeze-dried sediments were extracted for FTICR-MS analysis following a previously reported procedure.[6, 7] In brief, approximately 2.0 g of dry, homogenized sediment was extracted five times by ultrasonication with 10 mL of 9:1 (v/v) dichloromethane/methanol at ambient temperature, for 30 min. The extracts were dried over anhydrous sodium sulfate, and the combined extracts were rotary evaporated to approximately 10 mL. Small aliquots of the extracts were blown dry under a N_2 stream and then reconstituted in toluene to a final concentration of 1.25 mg/mL.

2.3. FTICR-MS Analysis

Sediment extracts were analyzed using a 12 T Bruker SolariX mass spectrometer (Bruker, MA, USA) with APPI-P (atmospheric pressure photoionization in positive ion mode) as the ion source. Sample solutions were infused into the ion source using a syringe pump set to deliver 200 µL/h. A krypton lamp at 10.6 eV was used for sample ionization. The transfer capillary temperature and nebulizer pressure were set to 400°C and 1.5 bar, respectively. Previous studies of biological molecules using APPI under thermospray conditions showed negligible in-source thermal degradation.[6, 7, 13] The APPI-P technique allows the detection of analyte components as protonated and/or radical ion species. Ions formed depend on the proton and electron affinities of the dopant relative to the analyte. With a toluene dopant, if the proton

affinity of the analyte is higher than the proton affinity of the benzyl radical, a protonated molecule can form. If the electron affinity of the toluene radical cation is higher than the electron affinity of the analyte (lower or equal ionization energy than toluene) a radical molecular ion can form (Purcell et al., 2006). In this paper, radical species will be denoted with • symbol, for example hydrocarbon radical ions will be labelled as HC•, in contrast to protonated ones, which labels do not contain the bullet symbol - for example, HC stands for protonated hydrocarbons, as described in previous studies.[14]

The FTICR-MS instrument is regularly tuned using reference calibration mixtures; other quality assurance steps include the addition of internal standard compounds to ensure mass spectra accuracy, as well as acquisition of appropriate blank samples with every batch of samples analyzed.[6, 7] Ions ranging from *m/z* 150 to 1500 were isolated by a linear quadrupole and accumulated over 30 ms in the collision cell, before being transferred to the ICR cell. For each sample, 200 transients of 8 million points in the time domain were collected over 12 min (0.2 h) and summed to improve the experimental signal-to-noise ratio. Approximately 50 µg of the whole sediment extract is consumed in one FTICR-MS analysis (200 µL/h × 0.2 h × 1.25 µg/µL). FTICR-MS raw data were processed using the CaPA software package (Aphorist Inc., Calgary, AB, Canada). The compositional boundaries were set to $C_{4–95}H_{0–200}N_{0–4}S_{0–1}O_{0–12}P_{0–1}$. The double-bond equivalent (DBE) range, which is a measure of hydrogen deficiency in a molecule due to double bonds and/or cyclic structures, was set between 0 and 60. Peaks with a signal-to-noise ratio higher than 4 were assigned, based on highly accurate mass measurements (mean peak assignment error ~100 ppb) and the comparison of isotopic patterns with the theoretical isotopolog distributions, whenever possible. Any peak detected in the solvent blanks with relative

intensity higher than 1% of the base peak had their intensities set to zero in sample spectra. It is important to note that although FTICR-MS analysis results in unambiguous molecular formula assignments, the exact structural identity of the peaks cannot be established without additional experiments, such as tandem mass spectrometry (MS/MS). However, characteristic carbon number and DBE distributions can be used as a strong indication of the inferred molecular structures, particularly for the known and well-studied classes of biomarker species where we have enough prior experience and literature reports.

The Ragnarök software package (Aphorist Inc., Calgary, AB, Canada) was employed for data analysis and visualization of assigned molecular formulae; this software features advanced capabilities to treat and visualize various layers of molecular information embedded in the FTICR-MS outputs, that allow grouping and averaging of multiple samples, and their general compositional parameters (e.g., heteroatom composition, average carbon numbers and DBE, etc.). In this study, we focus only on spatial variability among different sampling sites, and therefore we used this software feature to group and average out all the samples collected at the same site, regardless of the sampling season. Albeit some temporal differences (January to May) in geochemical fingerprint can be observed at the four sampling sites, they are less prominent, and therefore will not be discussed herein, but in future reports.

Finally, due to variable ionization responses and efficiencies among the many diverse species detected, FTICR-MS analyses are inherently semiquantitative, and are not an expression of species' absolute concentration. Therefore, all the discussions and calculations relating to intensity/abundance of compound classes, and/or putative molecular markers should be viewed in relative terms, wherein the intensity is normalized to the sum of all assigned peaks in

the analyzed sample (labelled as "% of Sample" on y-axes in the visualization plots). Notwithstanding, because the same concentrations of sediment extract are injected into the instrument, these relative intensities can be used to make relevant comparisons, both within a specific sample, as well as between the samples analyzed in the same batch.

Principal component analysis (PCA) using relative intensity of compound classes as variables was performed and visualized with the *FactoMineR package of R statistical software.*[15]

3. Results and Discussion

3.1. Overall compositional trends

Figure 2 shows general compositional trends of surface sediments at four sampling sites, derived from FTICR-MS analysis, including heteroatom (N, S, O) ratios relative to carbon, and average carbon number and double bond equivalent (DBE) values. The values are averaged over different sampling periods, as commented in the Section 2.3., and normalized to unitary scale for better comparison.

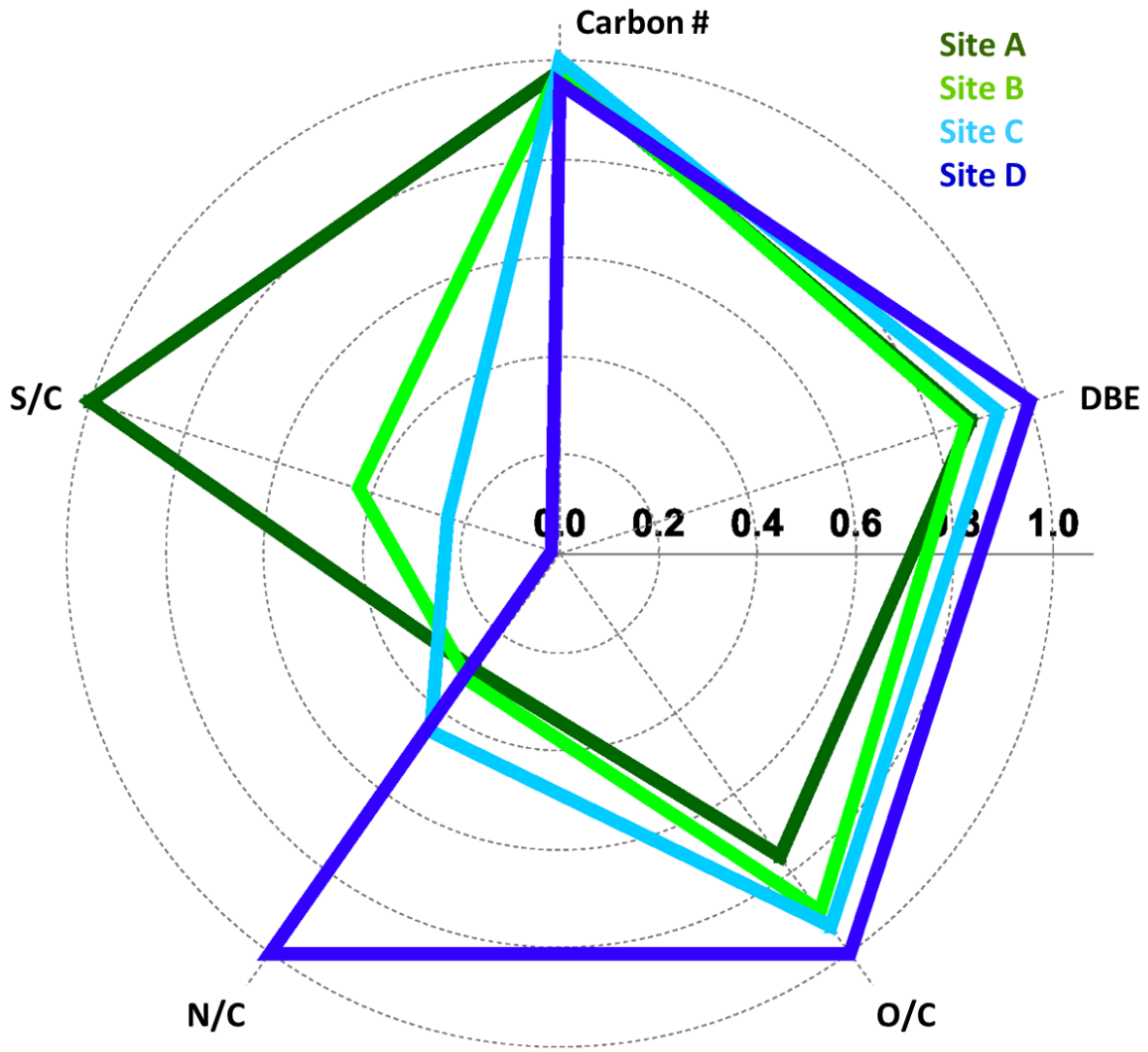

200

201 **Figure 2.** Radar plots showing the averaged and normalized FTMS-derived compositional parameters
202 including heteroatom (nitrogen, sulphur, and oxygen) to carbon ratios, carbon number and double-bond
203 equivalent, at the four sampling sites along the sampling transect - from freshwater, terrestrially
204 influenced site A to saline site D in the coastal South China Sea.

205 The most notable observation from Fig. 2 is that the site A, which is the most proximal to the
206 mouth of the Pearl River, has the highest S/C ratio, while on the other hand the most distal site
207 D has the highest N/C and O/C ratio, which likely indicates a shift in the nature of organic

matter from terrestrial-influenced to marine, in line with what was previously observed in the Pearl River estuary and in other examples of river-coastal sea interface environments. [12, 16] Furthermore, there is a trend towards more unsaturated species (i.e. with more rings and/or double bonds) as we move to sites C and D, possibly reflecting a more recent, i.e. "fresh", and less reworked character of organic matter sourced from marine organisms.[17, 18]

Looking at the distribution of compound classes, Fig. 3, main compositional differences are characterized by a decreasing relative abundance of HC classes (both radical and protonated) and sulphur-bearing species (SO_x and S classes) going from the site A towards the more distal sites (B, C, D), with a concomitant increase in relative abundance of oxygen classes (O_3 through O_6) and nitrogen classes (NO_x and N_4O_x). In the following sections we explore the main molecular features of species comprising some of the most abundant, representative compound classes.

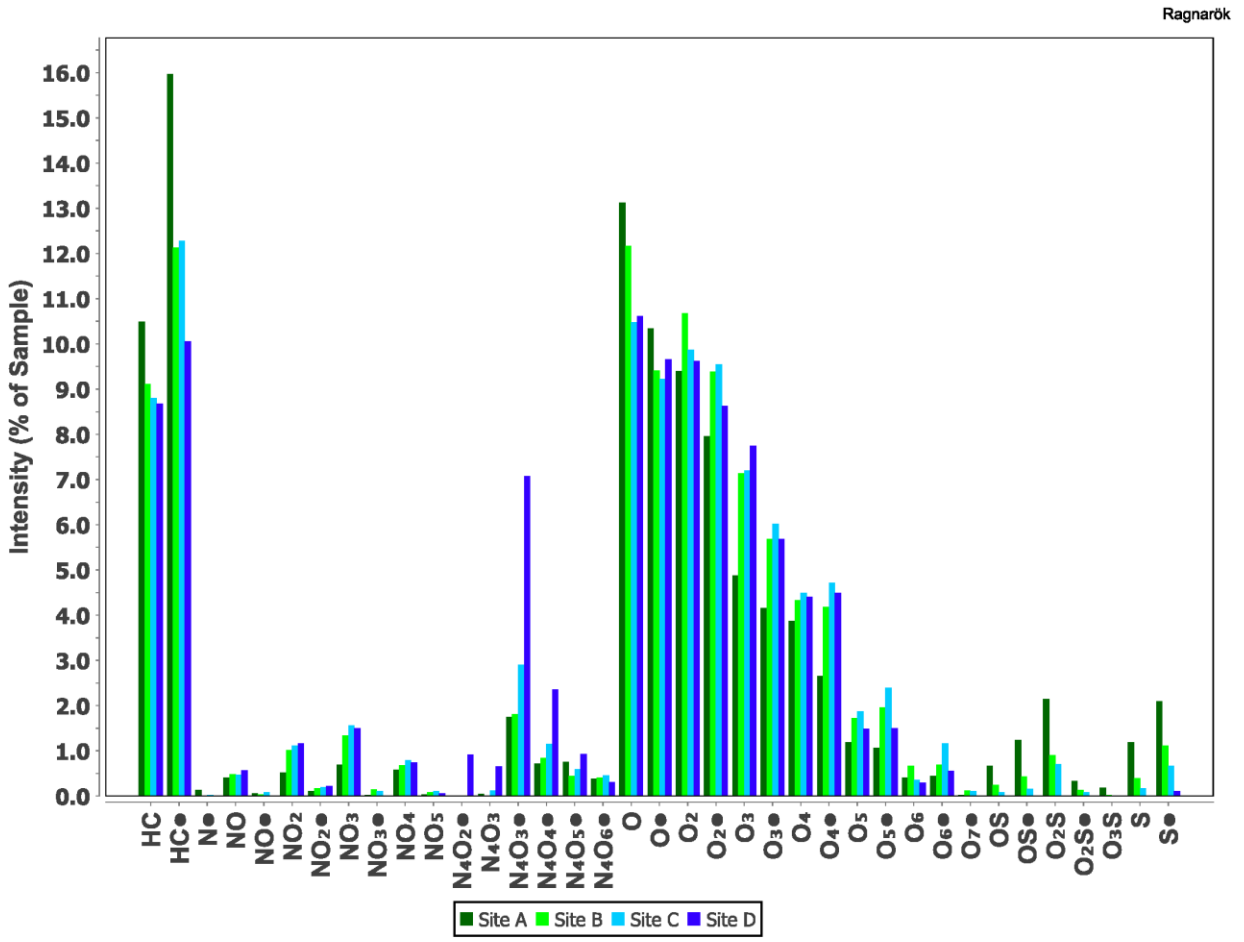

220

221 **Figure 3.** APPI-P FTICR-MS heteroatom class distribution is surface sediments at four sampling sites
222 analyzed in this study. Dots following class labels refer to radical ions (odd electron ion) while the
223 absence of a dot refers to protonated ions (even electron ion).

224 ### 3.2. Hydrocarbon compound classes

225 Hydrocarbon compound classes, including both the radical (HC) and protonated (HC•) ion
226 species, are highly prominent at the river discharge site A, followed by a decrease in relative
227 intensity, by some 3 to 6%, as one moves towards the coastal SCS, Fig. 3 (herein, we discuss
228 only radical HC class; protonated HC• species shows similar overall composition). Plot of DBE
229 groups distribution within the HC class, Fig. 4 (A), reveals further differences between the site

A, at which HC species with DBE 5 and 6 have the highest relative intensity, and the rest of the sampling sites, where DBE relative intensity maxima shifts to 6 and 7, suggesting the presence of somewhat more unsaturated species.

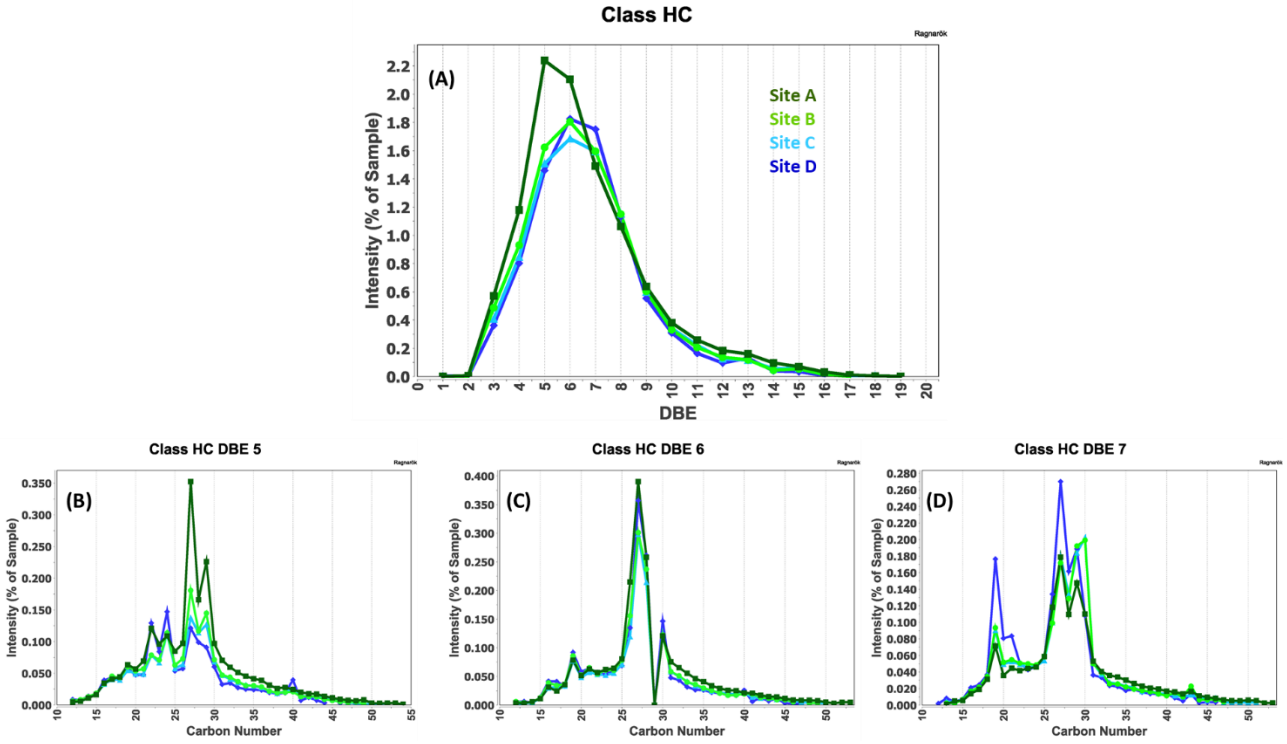

Figure 4. Distribution of (A) double bond equivalents (DBE) within HC compound class, and (B-D) carbon pseudohomolog distributions of the most abundant DBE (5-7) groups.

Within DBE 5 group, pseudohomologs with 27 and 29 carbon atoms are the most prominent at the riverine-influenced site A, and their relative intensity progressively decreases towards site D, concomitantly with a relative enrichment of C_{22} and C_{24} pseudohomologs. We putatively assign these DBE 5 species as sterenes, see insert in Fig. 5(A), (poly)unsaturated metabolites of sterols. Sterols are ubiquitous biomolecules, occurring naturally in most of the living organisms, including terrestrial plants, phytoplankton, bacteria, and algae.[19, 20] Sterols have also been used

to monitor anthropogenic organic matter fluxes, such as sewage inputs to coastal waters.[21] Early diagenetic transformation of sterols to sterenes in particulate and sedimentary organic matter has been documented,[22, 23] which is typically a first stage in a longer term process of their transformation to triaromatic steroids and steranes, occurring during organic matter maturation on geological timescales.[24] The only report of direct biogenic sourcing of sterenes in marine environments has been related to a specific cholesta-3,5-diene found in surface waxes of isopod *Ligia oceanica*.[25] Herein we observe a diverse geochemical composition of putative sterenes, which is more in line with complex diagenetic processes likely related to a broader pool of source endmembers.[23, 26] Notwithstanding the specific source(s), there is a strong correlation of shorter chain sterenes to increasing salinity, Fig. 4; therefore, based on the observations within DBE 5 group of HC class, we propose that an increasing ratio of short- (C_{22}+C_{24}) to long-chain (C_{27}+C_{29}) sterenes (abbreviated as SLS), can be used to distinguish the transition between terrestrial and marine environments in modern sediments of Pearl River estuary.

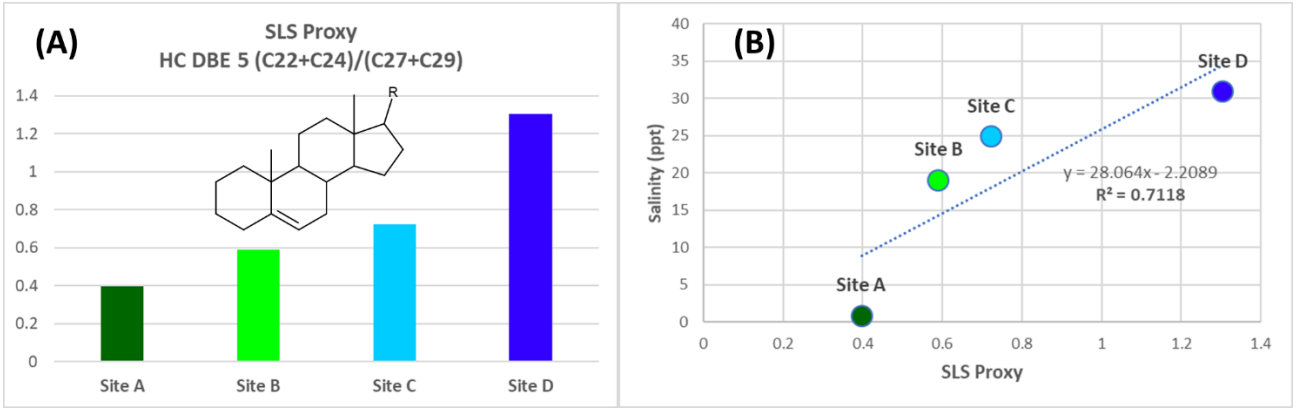

Figure 5. (A) Ratio of most prominent HC DBE 5 species, tentatively identified as short- and long-chain sterenes (SLS), at four sampling sites. Insert shows a generalized structure of putative sterenes, where R

259 denotes a side alkyl substitutions of variable carbon length. Y-axis denotes the ratio of the selected
260 species (B) Short- and long-chain sterenes (SLS) proxy as a function of seasonally averaged salinity at
261 four sampling sites.

262 In the DBE7 group, there is an increased relative intensity of C_{19}, C_{21} and C_{27} pseudohomologs at
263 the distal site D, compared to other locations, Fig. 4(D). Finally, within DBE 6, Fig. 4(C), species
264 with 19, 27 and 30 carbons in their formulae, are most abundant; however, no significant
265 differences in molecular distribution between sampling sites are observed. In terms of putative
266 identification, these species are possibly polyunsaturated sterol derivatives, such as dienes and
267 trienes.[22]

268 ### 3.3. Oxygen-containing compound classes

269 Within the oxygen bearing species, an overall trend is that the intensity of single oxygen class
270 (O), both radical and protonated, decreases from site to A to site D, while more oxygenated
271 compound classes (i.e., O_2 through O_6) tend to be more abundant in the transition zone (sites B
272 and C) and marine-influenced site D, Fig. 3.

273 Within compound class O, we observe that DBE 1 species dominate at site A, with
274 approximately 2.6% relative intensity, and become gradually less abundant towards site D, Fig.
275 6(A). The relative intensity of DBE 6-7 molecules is dominant at site D, compared to the other
276 locations, indicating an increased presence of more unsaturated oxygen species in the marine
277 setting. Carbon distribution within the DBE 1 species, Fig. 6(B), exhibits a prominent odd-to-
278 even distribution in the $C_{30\text{-}36}$ range, where $C_{31,33,35}$ species abound at the riverine site A, and

279 then progressively decrease in relative intensity at sites B, C and D, clearly tracking the shifting
280 trend of salinity and other environmental parameters along the sampling transect.

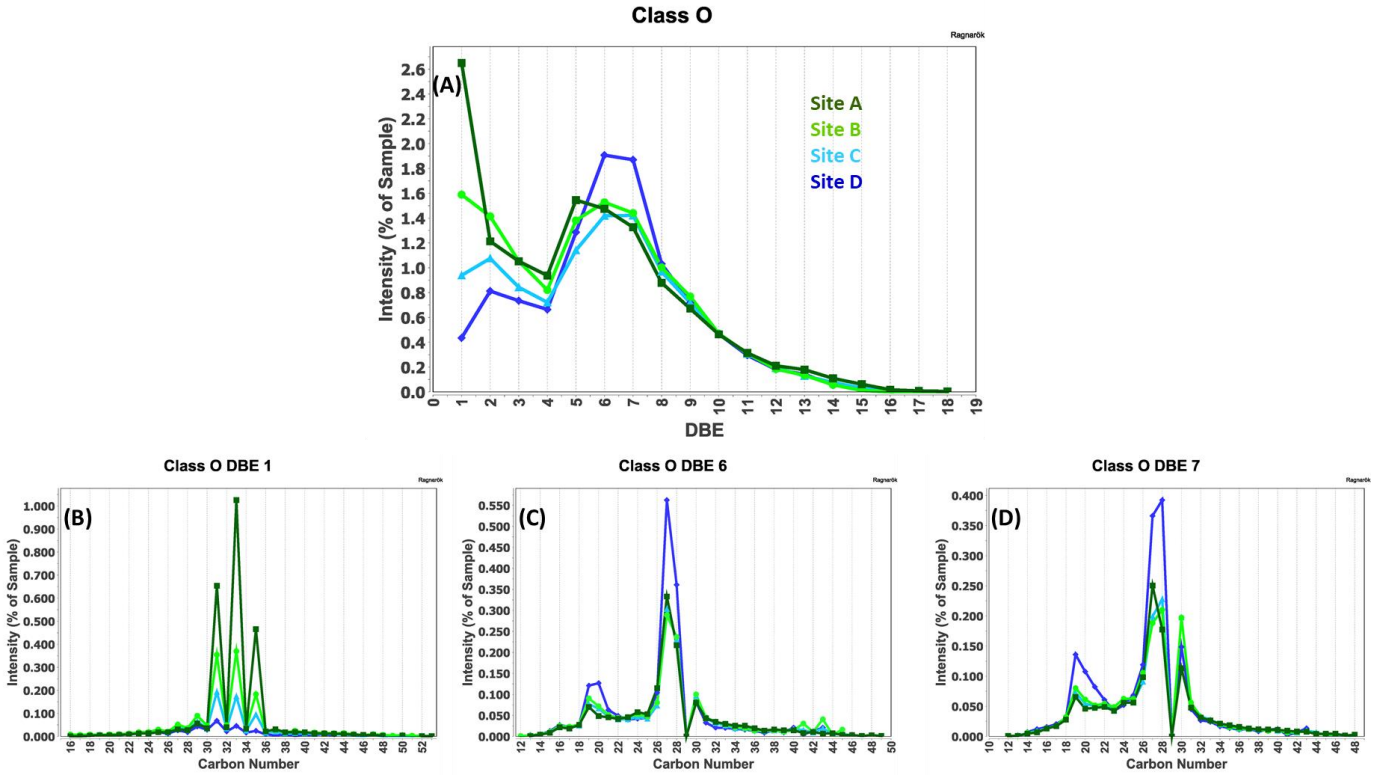

281

282 **Figure 6.** Distribution of (A) double bond equivalents (DBE) within O compound class, and (B-D) carbon
283 pseudohomolog distributions of the most abundant DBE groups.

284 Long chain (C_{37-39}) unsaturated alkyl ketones (alkenones) are well-known biomarkers found in
285 both freshwater and marine sediments.[27, 28] We hypothesize that C_{31}, C_{33}, and C_{35} species with
286 DBE 1, are fully saturated, shorter chain alkenone analogues.[29] Previous reports have found
287 such saturated species termed alkanones, in thermally altered sediments, with carbon chains in
288 the C_{11-33} range.[30] Also, hydroxy alkanones are often reported in different marine settings
289 wherein the postulated formation pathways include the oxidation of *n*-alkyl diols or hydrolysis
290 of complex mid-chain functionalized polymers.[31-33] Based on that, we hypothesize that putative

291 $C_{31\text{-}35}$ alkanones we detected in this study are also likely diagenetic (by)products of more
292 functionalized alkyl species. Unambiguous confirmation of their origin is not possible with the
293 data at hand and would require additional targeted studies. However, at a minimum,
294 observations from this study suggests that these putative alkanone species seem to have proxy
295 potential in distinguishing terrestrial-influenced and/or freshwater zones within Pearl River
296 estuary.

297 The distribution of DBE 6 and 7 species show prominent peaks at C_{19}, C_{20}, C_{27}, C_{28} and C_{30}, Fig.
298 6(C) and (D), likely related to the sterene species observed in hydrocarbon class (Section 3.3),
299 wherein species detected in O compound class are possibly precursor molecules in the
300 diagenetic sequence that produces sterenes observed in HC class.[24] It has been reported that
301 the Changjiang River acts as a conduit of terrestrially-sourced sterols into the East China sea,[34]
302 therefore, it is not implausible that our observations points to a similar process happening in
303 the Pearl River estuary.

304 A decreasing ratio of DBE 1 over DBE 6 and 7 seen in species in the compound class O can be
305 proposed as a proxy of the shift from freshwater to saline/marine setting, Fig. 7.

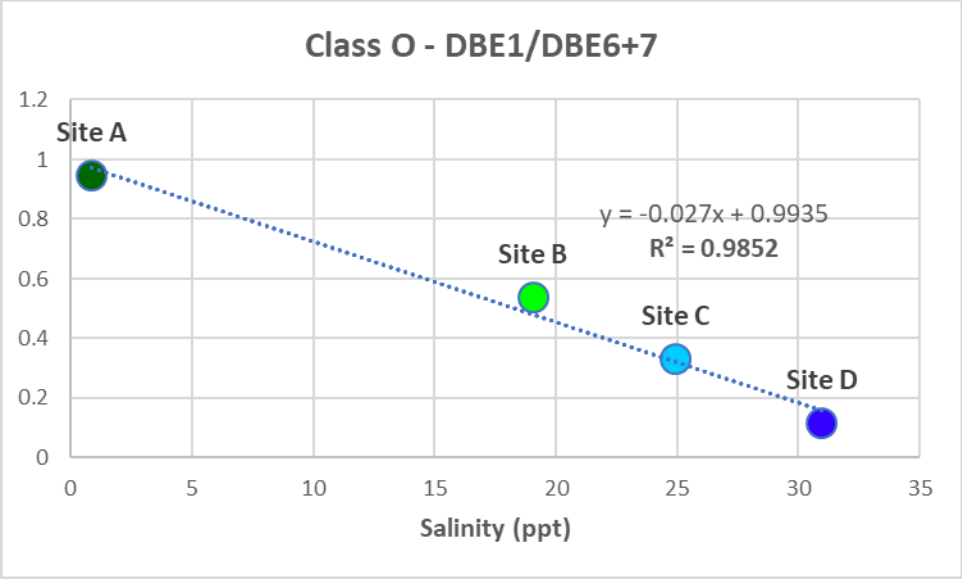

306

307 **Figure 7.** Cross-plot of salinity and the ratio between DBE 1 and DBE 6 and 7 species within the

308 compound class O. Y-axis denotes the ratio of the selected species.

309 Heteroatom class O_2, most notably shows increased relative intensity of DBE 2 species, more so

310 at the sites A and B and somewhat less at the marine site D, as well as relative preference of

311 DBE 7 and 8 groups at sites B, C and D, relative to site A, Fig. 8(A).

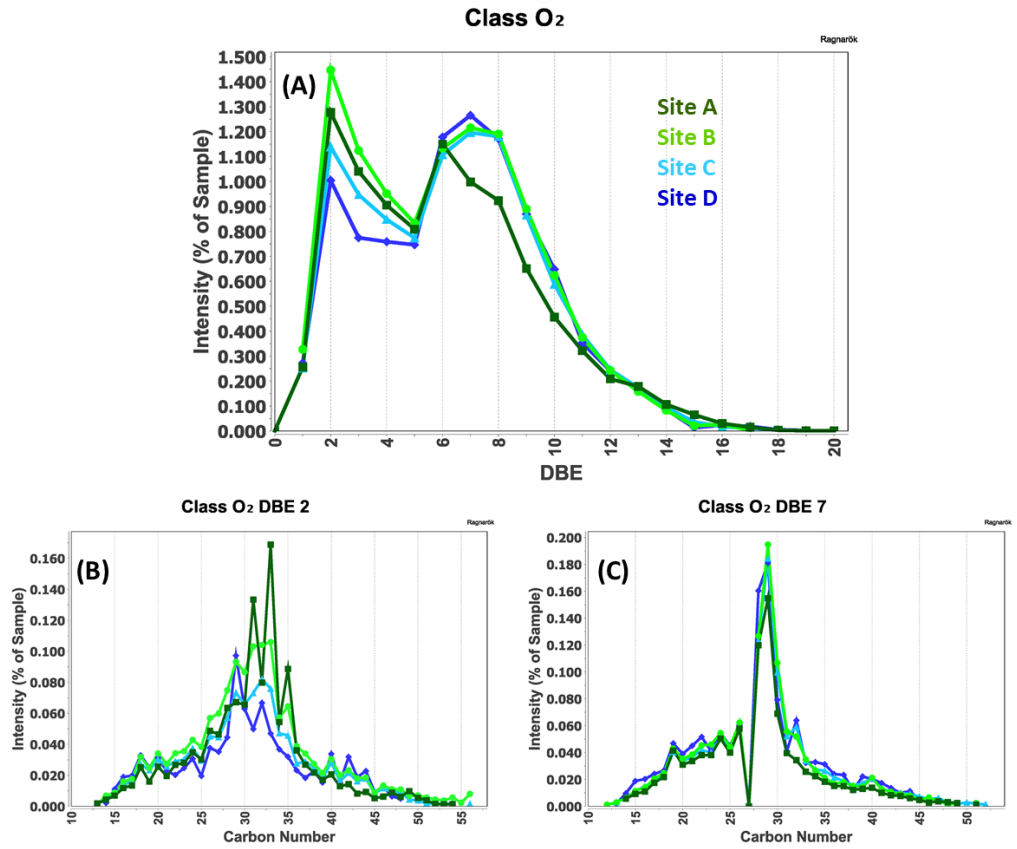

Figure 8. Distribution of (A) double bond equivalents (DBE) within the O_2 compound class, and (B-C) carbon pseudohomolog distributions of the most abundant DBE groups.

Within DBE 2 group of the class O_2, Fig. 8(B), we observe a clear separation of riverine site A, dominated by the odd-to-even distribution of C_{31}, C_{33} and C_{35} carbon pseudohomologs, and marine site D with notable peaks at C_{29}, C_{32}, as well as at C_{40} and C_{42}, while carbon distribution at sites B and C represents an intermediate/mix of A and D compositional endpoints. Class O_2 DBE 2 species have been identified in previous FTICR-MS studies of biodegraded petroleum reservoirs as naphthenic acids; however in the case of petrogenic naphthenic acids, the carbon distribution is uniform, i.e., Gaussian-like.[35] This "smoothing-out" of geochemical fingerprints is what is typically observed in crude oil samples, where the original fingerprint of source fossil

organic matter is made uniform by catagenetic processes occurring over geological timescales.[36-39] However, in the case of sediments analyzed in this study there is a very pronounced preference in carbon distributions of the molecular markers detected, characteristic of relatively recently deposited organic matter found in modern sedimentary environments,[40] as exemplified herein by the odd-to-even, $C_{31\text{-}35}$ carbon sequence within the DBE 2 group of O_2 compound class. Therefore, possibly a more plausible identity of these species would be long chain di-ketones, i.e., diones, analogs of well known alkenones, and related to C_{31}, C_{33}, and C_{35} species in the DBE 1 group of compound class O (as discussed above). We did not find any reports of long chain alkane dione species in recent sediments, therefore at this point, without further targeted, confirmatory studies, we only propose this chemical identity to the community as a working hypothesis. In support of that hypothesis, we note several studies that reported degradative oxidation of other organic species in sediments, both xenobiotic such as polycyclic aromatic hydrocarbons,[41, 42] and biogenic, such as triterpenoids,[43] to their dione analogs. Similarly, it is possible that C_{31}, C_{33}, and C_{35} species of the DBE 1 group in O class are transformed via oxidation to their analogous carbon pseudohomologs in the DBE 2 group of O_2 compound class. Regardless of their origin, we can use these characteristic carbon distributions in DBE 2 group of compound class O_2 to distinguish between terrestrially- and marine-related organic matter in the sediment, Fig. 9.

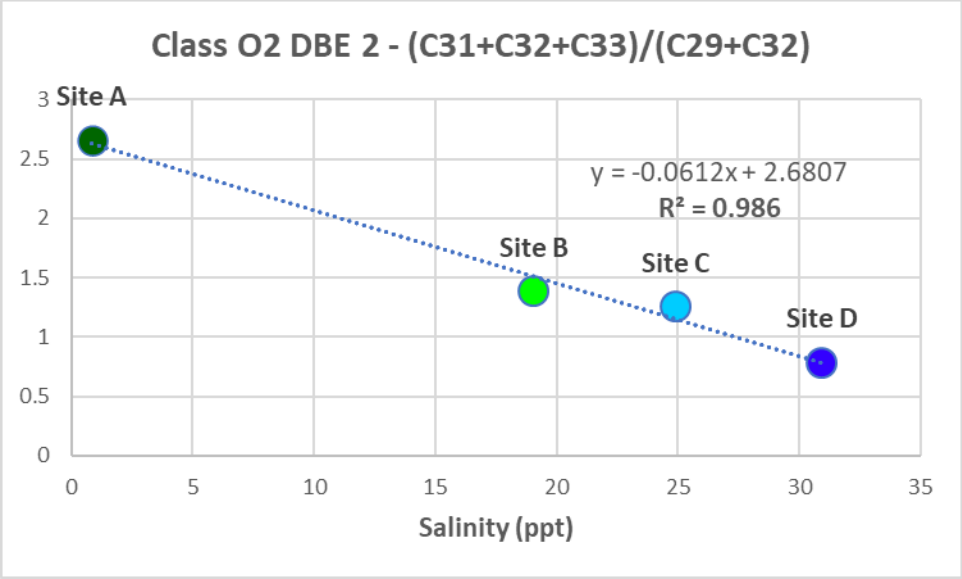

341

342 **Figure 9.** Cross-plot of salinity and the ratio between $C_{31\text{-}33}$ and C_{29}/C_{32} pseudohomologs within DBE2

343 species of the compound class O_2. Y-axis denotes the ratio of the selected species.

344 Heteroatom class O_3 features prominent DBE 2,7 and 8 species, Fig. 10(A), with site A having

345 comparatively lower relative intensity of O_3 species compared to other sampling locations,

346 especially site D, Fig. 3. The most distal location D also stands out in terms of prominent carbon

347 pseudohomolog peaks within those DBE groups, namely C_{19}, $C_{33\text{-}35}$ within DBE 2; C_{24} and C_{27} in

348 DBE 7, and C_{24}, and C_{28} in DBE 8.

349

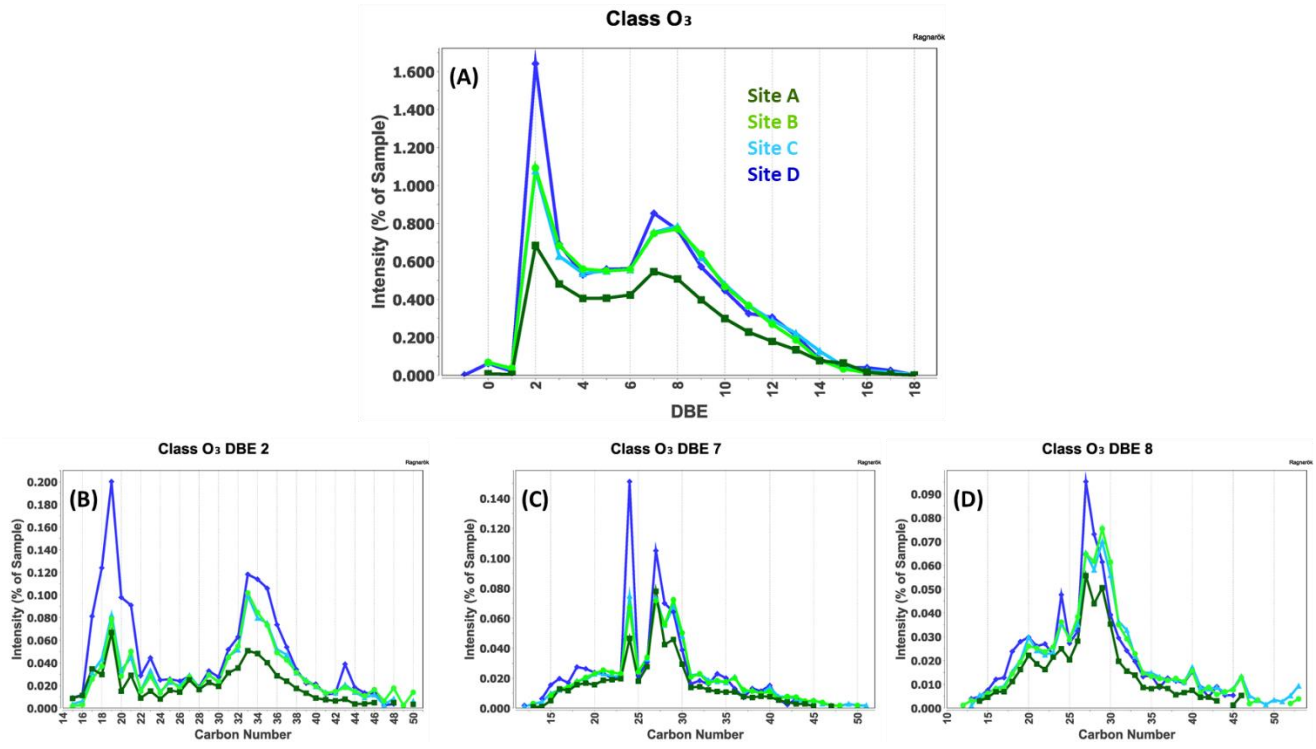

Figure 10. Distribution of (A) double bond equivalents (DBE) within the O3 compound class, and (B-D) carbon pseudohomolog distributions of the most abundant DBE groups.

Finally, we note a common feature in all the oxygen classes discussed in this section, namely the presence of indicative peaks in the 40-45 carbon range, across diverse DBE groups, see Fig. 6(C) and Fig. 8(B) as illustrative examples. We have previously reported C_{40} species in both recent sediments and immature crude oils and related them to carotenoid pigments.[7, 39] We hypothesize that the C_{40} species detected in this study may also be related to carotenoids and their alkylated derivatives.

3.4. Nitrogen-containing compound classes

Among compound classes that contain nitrogen, most abundant are the NO_x (x=1-5) and $N4O_X$ classes (x=2-6), Fig. 3. Class NO_{2-6} species with DBE 1-6 have been previously reported in marine

sediments collected in the Gulf of Mexico,[7] with resembling molecular properties to NO_x species detected in this study, Fig. 11.

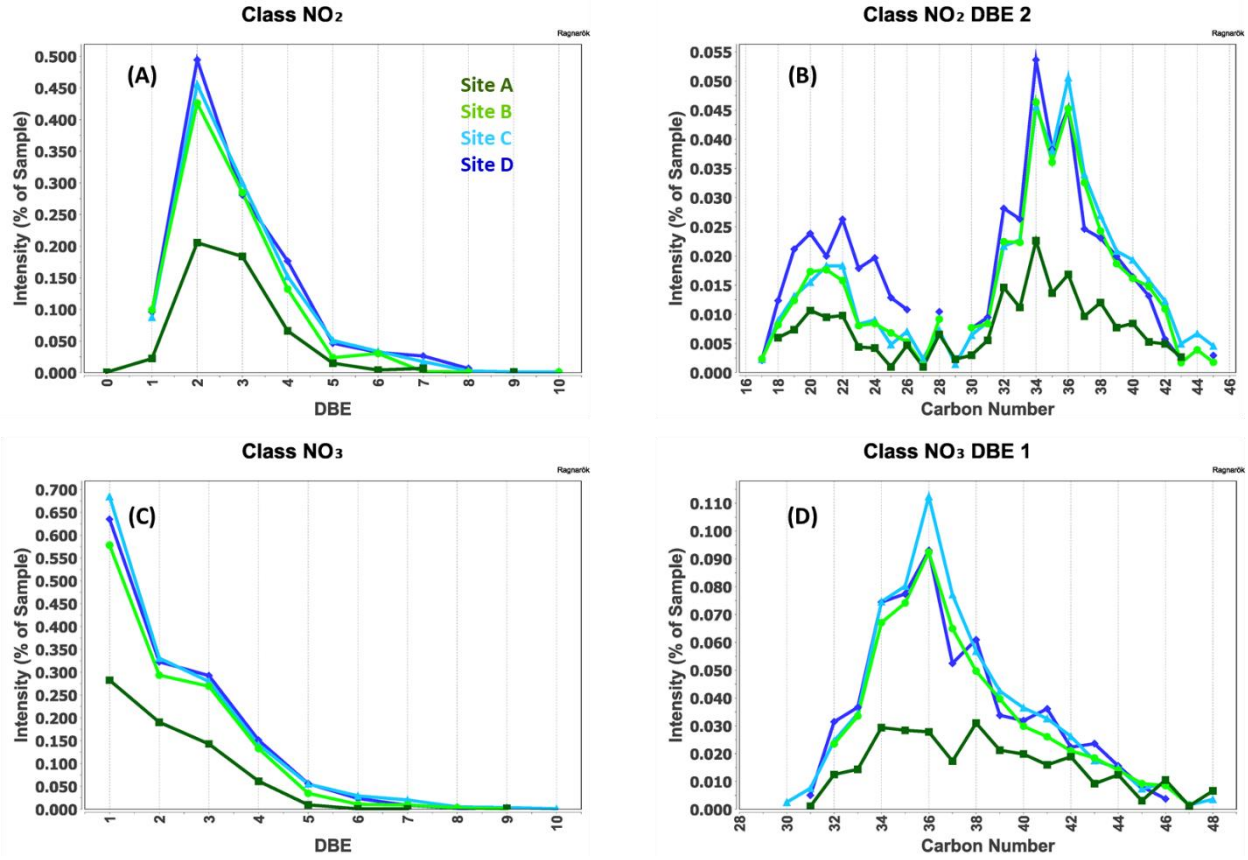

Figure 11. Distribution of (A and C) double bond equivalents (DBE) within NO_2 and NO_3 compound class, and (B and D) carbon pseudohomolog distributions of the most abundant DBE groups within those compound classes.

These species have been related to structural lipids of various (micro)organisms;[7] in particular, we highlight a recent lipidomics mapping of sphingolipids in marine microalgae.[44] Sphingolipids are chemically and functionally diverse group of membrane lipids, many of which include NOx moieties in their molecular structure, bound to long alkyl chains.[45] Common microalgae phyla such as *Bacillariophyta*, *dinophyta* and *haptophyte*, are abundant in coastal estuarine and

deltaic environments, such as found in the northern SCS and Gulf of Mexico,[46, 47] and could be the sources of sphingolipid or analogous species found in sediments from those coastal environments, as reported herein, and in our previous work.[7]

As for the $N4O_x$ species, we putatively identify them as tetrapyrrole phaeopigments, metabolites of phytoplankton chlorophyll pigments. Figure 12 shows carbon pseudohomolog distribution of DBE 20 species within N_4O_3• compound class wherein C_{53} and $C_{32\text{-}34}$ are indicative of phaeophytin and pheophorbide chlorophyll metabolites, respectively.[7, 48]

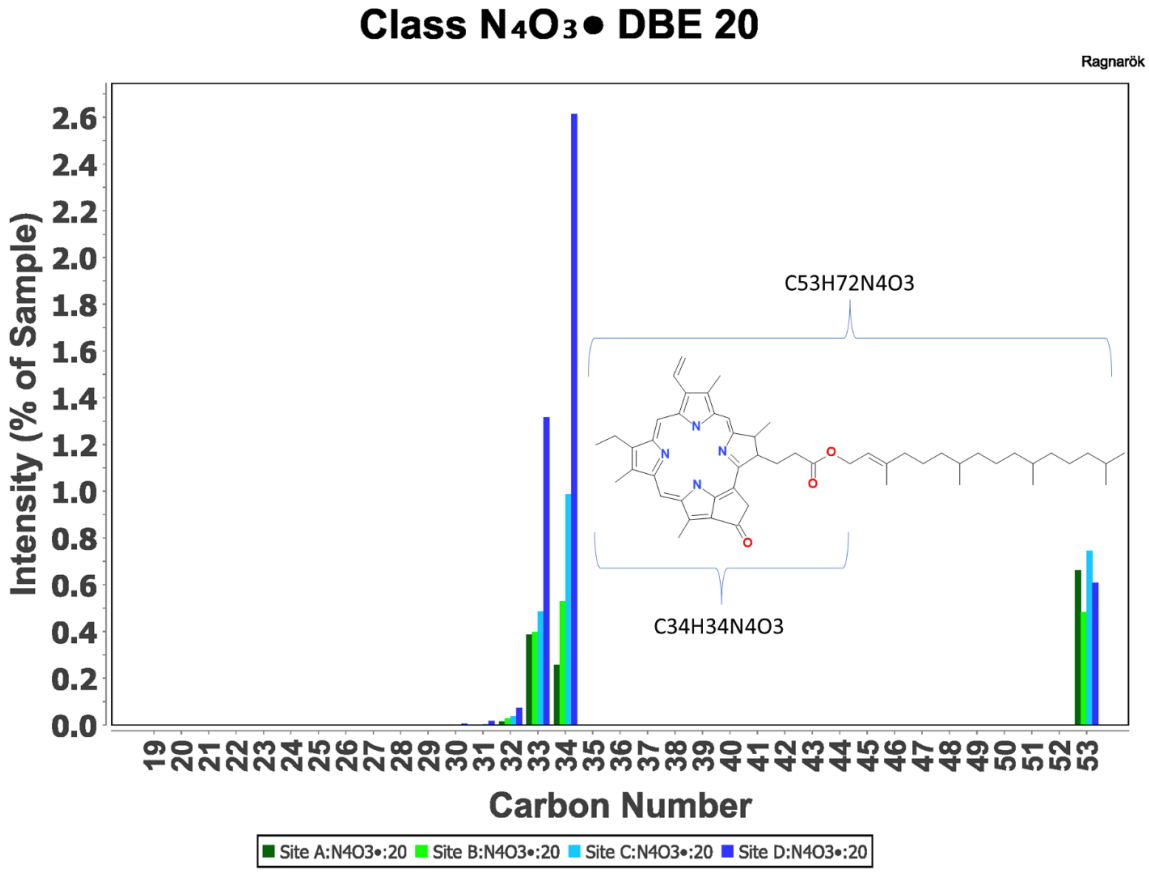

Figure 12. Carbon pseudohomolog distribution of DBE 20 species withing N_4O_3 class. These species are identified as phaeophytin (C_{53}) and pheophorbide ($C_{32\text{-}35}$) analogs, metabolites of phytoplankton chlorophyll pigments, example structures of which are shown in the figure insert.

There is likely a geochemical relationship between various N_4O_x species, for example the C_{34} pseudohomolog in the N_4O_3• class is probably produced by a hydrolytic cleavage of the side chain in the C_{53} pseudohomolog,[7, 48] see insert in the Fig. 9. Ratios between relative intensities of C_{34} and C_{53} N_4O_3• species increases towards site D, probably due to higher inputs of marine phytoplankton detritus, leading to accumulation of diagenetically more stable C_{34} phaeopigment in the sediment.[7, 48] Therefore, this ratio can serve as a proxy of transition to marine-like environment, from freshwater influenced setting within the estuary, Fig. 13.

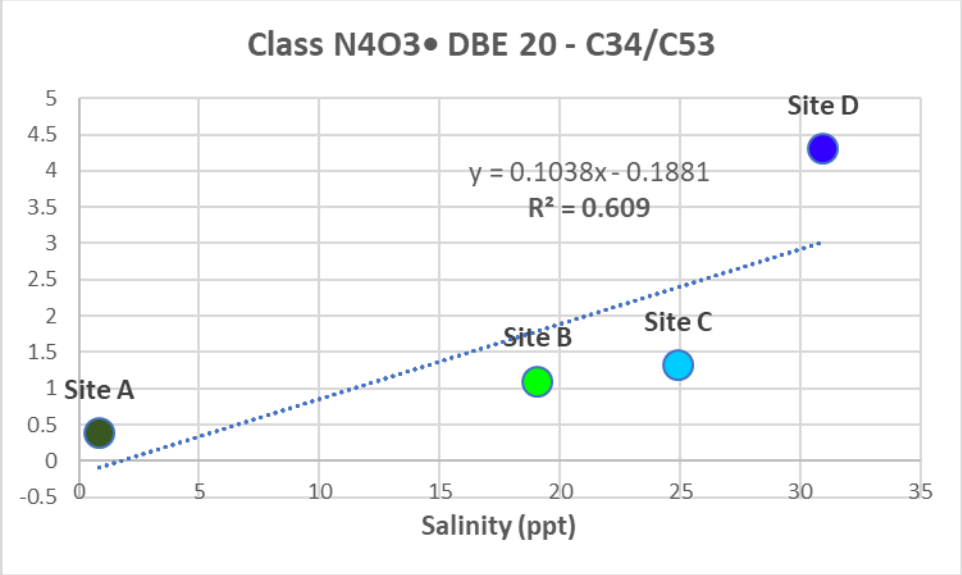

Figure 13. Cross-plot of salinity and the ratio between C_{34} and C_{53} pseudohomologs within DBE20 species of the compound class N_4O_3•. Y-axis denotes the ratio of the selected species.

3.5. Sulphur-containing compound classes

Sulphur species in the analyzed sediments were detected in both protonated and radical form as single sulphur-bearing compounds, as well as molecules with SO_x (x=1-3) functional groups, Fig. 3. Their relative intensity decreases from site A to site D, indicating a geochemical relationship with the Pearl River discharge. For example, the sulphur compound class is

dominated by the species with DBE 6, 9, and 12, Fig. 14(A) - such DBE distribution is a strong indication for the presence of thiophene compounds (DBE 6 - benzothiophenes, DBE 9 – dibenzothiophenes, DBE 12- benzonaphthothiophenes) of petrogenic origin,[14, 35, 49] suggesting the input of petroleum-derived pollution from the heavily populated and industrialized downstream portion of the Pearl River watershed. The presence of anthropogenically-sourced polycyclic aromatic hydrocarbons, including related thiophene compounds, in the Pearl River delta and estuary is well documented, and points to preferential partitioning of these species to particulates and sediment.[50-53]

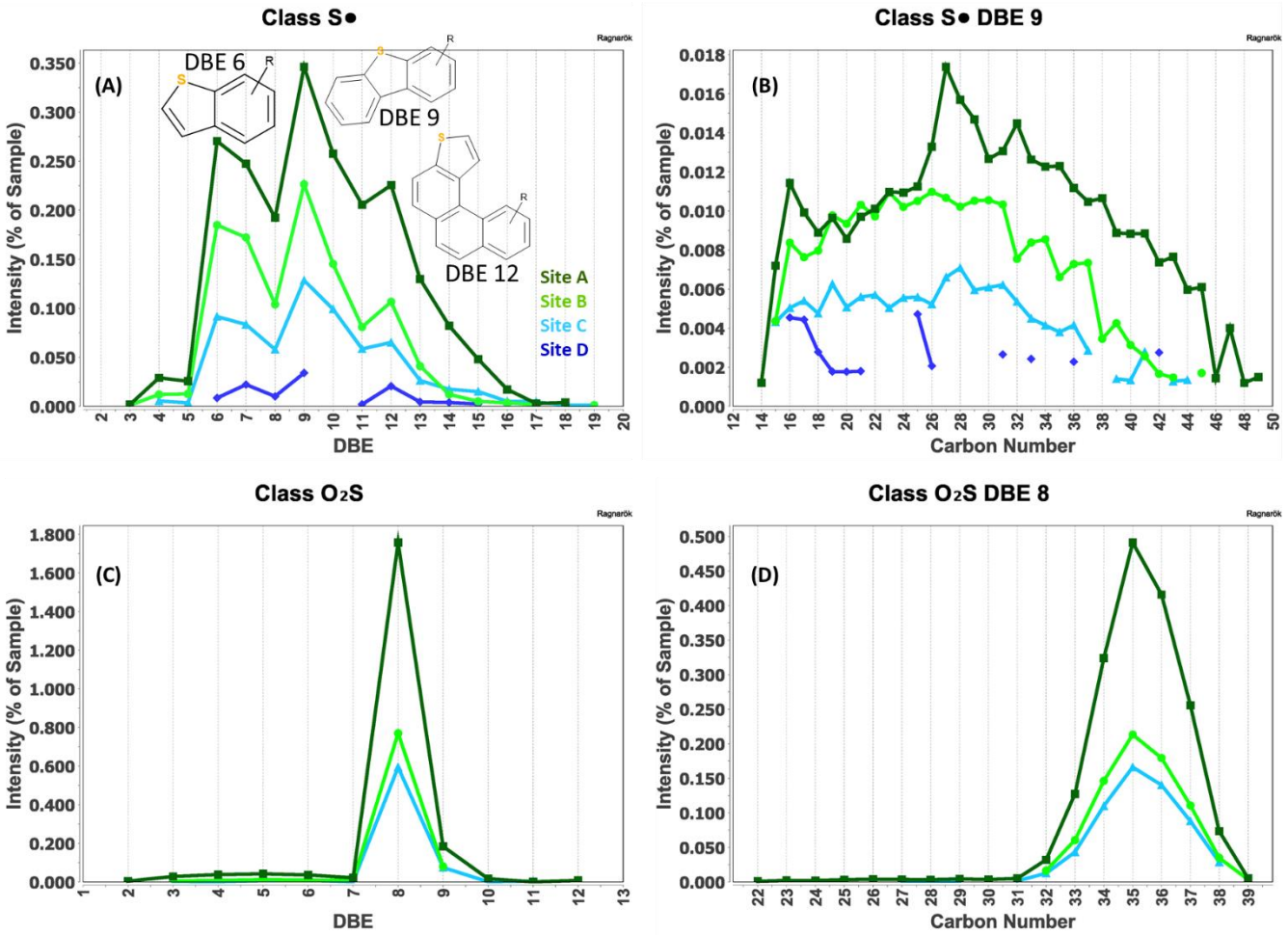

Figure 14. Distribution of (A and C) double bond equivalents (DBE) within S• and SO_2 compound class,

409 and (B and D) carbon pseudohomolog distributions of the most abundant DBE groups within those
410 compound classes. Inserts in the panel A represent generalized, putative structures of alkyl-substituted
411 benzothiophenes, dibenzothiophenes, and naphtobenzothiophenes, as found in DBE 6, 9 and 12 groups,
412 respectively.

413 Previous studies of biodegraded crude oils have interpreted compound class O_2S as comprised
414 of acidic species, likely containing one sulphur and carboxyl functional group, or one sulphur
415 and two hydroxyl functional groups, that are degradation products of parent species found in
416 the S compound class.[35] However, such transformations of sulphur species would result in DBE
417 distributions of products that would be either same/similar as in S class (if only hydroxyl groups
418 are introduced) or increased by one DBE unit (in the case that carboxyl group is introduced). On
419 the contrary, herein we observe that O_2S class is dominated by specific species within DBE 8,
420 comprised mainly of C_{35} carbon pseudohomolog, Fig. 14(C and D). Such specificity is possibly
421 indicative of a unique source endmember, and/or organo-sulphur reaction pathway;[54-56]
422 however, with the data at hand we cannot speculate further on the origin of O_2S species in the
423 sediments analyzed in this study.

424 **3.6. Summary, implications, and future work**

425 This study offers a spatial snapshot of the biogeochemical complexity as found in the Pearl
426 River estuary and coastal South China sea, wherein the composition of surface sediments
427 clearly reflects two distinctive environments, Fig. S1. Site A is influenced by the freshwater
428 discharge of PR, and related inputs of terrestrial and anthropogenic organic species, while site D
429 bears geochemical traits of coastal marine system. Between these two endpoints, at sites B and
430 C, we find a type of transitional setting, with mixed geochemical fingerprints.

While these results offer a very exciting glimpse into a plethora of possible sources and fates of organic matter in the PR estuary and coastal SCS, we are cautious to not overinterpret them. Geochemical signals preserved in bottom sediments are just an integration of all the input endmembers, diverse microbial communities and degradation/transformation/transport processes occurring both in the overlaying water column and sediments themselves. To fully decouple these elements, future studies should integrate high resolution sampling of organics in particulate, dissolved and sedimented carbon pools, at key points along the Pearl River and in the coastal SCS, with comprehensive microbiological and geochemical analyses of those carbon fractions.

From the geochemistry perspective, results presented in this study illustrate the power of FTICR-MS and similar multi-proxy approaches, that are particularly suitable for complex environments such as estuaries, where we have extreme diversity and heterogeneity of sources and types of organic inputs. While in this study we analyzed modern biogeochemical setting, the same approach could be, in principle, applied to paleoenvironmental assessments. This study and previous reports from our and other groups [3, 4, 6-9] demonstrate that FTICR-MS methods afford a broad-ranging assessment of various functional and chemical types of organic species, including discoveries of new species with promising proxy potential. At the same time, we note and recognize existing limitations of this methodology, especially the lack of fully quantitative capabilities; therefore, we see a continuous need to develop and improve complementary analytical protocols, including fractionation schemes and targeted quantitative methods.

Acknowledgments

JRR, RCS, TBPO, and SRL acknowledge various sources of support that contributed to this work, including the Canada First Research Excellence Fund (CFREF), Canada Foundation for Innovation (CFI), the Natural Sciences and Engineering Research Council of Canada (NSERC) and Canada Research Chairs (CRC), Bruker Daltonics, Aphorist Inc., PRG group, the Shenzhen Key Laboratory of Geo Omics of Archaea (ZDSYS201802081843490) at the Southern University of Science and Technology, and the University of Calgary. We thank Wang J. and Captain Huang for helping with the sampling during the cruise. We kindly thank Priyanthi Weerawardhena, Melisa Brown, and Ryan Snowdon for their help with sample preparation, FTICR-MS analysis, and software support. This research was supported by the National Science Foundation of China (92051117 (WX), 41776137 (WX), 42141003 (CZ), and 91851210 (CZ)).

References

1. Liu, J.; Liu, X.; Wang, M.; Qiao, Y.; Zheng, Y.; Zhang, X.-H., Bacterial and archaeal communities in sediments of the north Chinese marginal seas. *Microbial ecology* **2015,** *70*, (1), 105-117.
2. Yu, Y.; Wang, H.; Liu, J.; Wang, Q.; Shen, T.; Guo, W.; Wang, R., Shifts in microbial community function and structure along the successional gradient of coastal wetlands in Yellow River Estuary. *European Journal of Soil Biology* **2012,** *49*, 12-21.
3. Alfken, S.; Wörmer, L.; Lipp, J. S.; Wendt, J.; Schimmelmann, A.; Hinrichs, K.-U., Mechanistic Insights Into Molecular Proxies Through Comparison of Subannually Resolved Sedimentary Records With Instrumental Water Column Data in the Santa Barbara Basin, Southern California. *Paleoceanography and Paleoclimatology* **2020,** *35*, (10), e2020PA004076.
4. Alfken, S.; Wörmer, L.; Lipp, J. S.; Wendt, J.; Taubner, H.; Schimmelmann, A.; Hinrichs, K.-U., Micrometer scale imaging of sedimentary climate archives–Sample preparation for combined elemental and lipid biomarker analysis. *Organic Geochemistry* **2019,** *127*, 81-91.
5. Law, K. P.; Zhang, C. L., Current progress and future trends in mass spectrometry-based archaeal lipidomics. *Organic Geochemistry* **2019,** *134*, 45-61.
6. Radović, J. R.; Silva, R. C.; Snowdon, R.; Larter, S. R.; Oldenburg, T. B., Rapid screening of glycerol ether lipid biomarkers in recent marine sediment using atmospheric pressure photoionization in positive mode Fourier transform ion cyclotron resonance mass spectrometry. *Analytical chemistry* **2016,** *88*, (2), 1128-1137.

7. Radović, J. R.; Silva, R. C.; Snowdon, R. W.; Brown, M.; Larter, S.; Oldenburg, T. B., A rapid method to assess a broad inventory of organic species in marine sediments using ultra‐high resolution mass spectrometry. *Rapid Communications in Mass Spectrometry* **2016,** *30*, (11), 1273-1282.
8. Wörmer, L.; Elvert, M.; Fuchser, J.; Lipp, J. S.; Buttigieg, P. L.; Zabel, M.; Hinrichs, K.-U., Ultra-high-resolution paleoenvironmental records via direct laser-based analysis of lipid biomarkers in sediment core samples. *Proceedings of the National Academy of Sciences* **2014,** *111*, (44), 15669-15674.
9. Wörmer, L.; Wendt, J.; Alfken, S.; Wang, J.-X.; Elvert, M.; Heuer, V. B.; Hinrichs, K.-U., Towards multiproxy, ultra-high resolution molecular stratigraphy: Enabling laser-induced mass spectrometry imaging of diverse molecular biomarkers in sediments. *Organic Geochemistry* **2019,** *127*, 136-145.
10. Zhang, S.; Lu, X. X.; Higgitt, D. L.; Chen, C.-T. A.; Han, J.; Sun, H., Recent changes of water discharge and sediment load in the Zhujiang (Pearl River) Basin, China. *Global and Planetary Change* **2008,** *60*, (3-4), 365-380.
11. Hou, P.; Eglinton, T. I.; Yu, M.; Montluçon, D. B.; Haghipour, N.; Zhang, H.; Jin, G. e.; Zhao, M., Degradation and Aging of Terrestrial Organic Carbon within Estuaries: Biogeochemical and Environmental Implications. *Environmental Science & Technology* **2021,** *55*, (15), 10852-10861.
12. He, B.; Dai, M.; Huang, W.; Liu, Q.; Chen, H.; Xu, L., Sources and accumulation of organic carbon in the Pearl River Estuary surface sediment as indicated by elemental, stable carbon isotopic, and carbohydrate compositions. *Biogeosciences* **2010,** *7*, (10), 3343-3362.
13. Bagag, A.; Giuliani, A.; Laprévote, O., Atmospheric pressure photoionization mass spectrometry of nucleic bases, ribonucleosides and ribonucleotides. *International Journal of Mass Spectrometry* **2007,** *264*, (1), 1-9.
14. Oldenburg, T. B. P.; Brown, M.; Bennett, B.; Larter, S. R., The impact of thermal maturity level on the composition of crude oils, assessed using ultra-high resolution mass spectrometry. *Organic Geochemistry* **2014,** *75*, 151-168.
15. Lê, S.; Josse, J.; Husson, F., FactoMineR: An R Package for Multivariate Analysis. *Journal of Statistical Software* **2008,** *25*, (1), 1 - 18.
16. Nasir, A.; Lukman, M.; Tuwo, A.; Hatta, M.; Tambaru, R.; Nurfadilah, The Use of C/N Ratio in Assessing the Influence of Land-Based Material in Coastal Water of South Sulawesi and Spermonde Archipelago, Indonesia. *Frontiers in Marine Science* **2016,** *3*, (266).
17. Zimmerman, A. R.; Canuel, E. A., Bulk Organic Matter and Lipid Biomarker Composition of Chesapeake Bay Surficial Sediments as Indicators of Environmental Processes. *Estuarine, Coastal and Shelf Science* **2001,** *53*, (3), 319-341.
18. Rossel, P. E.; Bienhold, C.; Hehemann, L.; Dittmar, T.; Boetius, A., Molecular Composition of Dissolved Organic Matter in Sediment Porewater of the Arctic Deep-Sea Observatory HAUSGARTEN (Fram Strait). *Frontiers in Marine Science* **2020,** *7*, (428).
19. McCallister, S. L.; Bauer, J. E.; Ducklow, H. W.; Canuel, E. A., Sources of estuarine dissolved and particulate organic matter: a multi-tracer approach. *Organic Geochemistry* **2006,** *37*, (4), 454-468.
20. Volkman, J. K.; Barrett, S. M.; Blackburn, S. I.; Mansour, M. P.; Sikes, E. L.; Gelin, F., Microalgal biomarkers: a review of recent research developments. *Organic Geochemistry* **1998,** *29*, (5-7), 1163-1179.
21. Martins, C. C.; Cabral, A. C.; Barbosa-Cintra, S. C.; Dauner, A. L. L.; Souza, F. M., An integrated evaluation of molecular marker indices and linear alkylbenzenes (LABs) to measure sewage input in a subtropical estuary (Babitonga Bay, Brazil). *Environmental Pollution* **2014,** *188*, 71-80.
22. Wakeham, S. G.; Gagosian, R. B.; Farrington, J. W.; Canuel, E. A., Sterenes in suspended particulate matter in the eastern tropical North Pacific. *Nature* **1984,** *308*, (5962), 840-843.
23. Gagosian, R. B.; Farrington, J. W., Sterenes in surface sediments from the southwest African shelf and slope. *Geochimica et Cosmochimica Acta* **1978,** *42*, (8), 1091-1101.

24. Mackenzie, A. S.; Brassell, S. C.; Eglinton, G.; Maxwell, J. R., Chemical Fossils: The Geological Fate of Steroids. *Science* **1982,** *217*, (4559), 491-504.
25. Hamilton, R.; Raie, M.; Weatherston, I.; Brooks, C.; Borthwick, J. H., Crustacean surface waxes. Part I. The hydrocarbons from the surface of Ligia oceanica. *Journal of the Chemical Society, Perkin Transactions 1* **1975**, (4), 354-357.
26. Wakeham, S. G., Steroid geochemistry in the oxygen minimum zone of the eastern tropical North Pacific Ocean. *Geochimica et Cosmochimica Acta* **1987,** *51*, (11), 3051-3069.
27. Marlowe, I. T.; Brassell, S. C.; Eglinton, G.; Green, J. C., Long chain unsaturated ketones and esters in living algae and marine sediments. *Organic Geochemistry* **1984,** *6*, 135-141.
28. Cranwell, P. A., Long-chain unsaturated ketones in recent lacustrine sediments. *Geochimica et Cosmochimica Acta* **1985,** *49*, (7), 1545-1551.
29. O'Neil, G. W.; Gale, A. C.; Nelson, R. K.; Dhaliwal, H. K.; Reddy, C. M., Unusual Shorter-Chain C35 and C36 Alkenones from Commercially Grown Isochrysis sp. Microalgae. *Journal of the American Oil Chemists' Society* **2021,** *98*, (7), 757-768.
30. Leif, R. N.; Simoneit, B. R. T., Ketones in hydrothermal petroleums and sediment extracts from Guaymas Basin, Gulf of California. *Organic Geochemistry* **1995,** *23*, (10), 889-904.
31. Méjanelle, L.; Laureillard, J., Lipid biomarker record in surface sediments at three sites of contrasting productivity in the tropical North Eastern Atlantic. *Marine Chemistry* **2008,** *108*, (1), 59-76.
32. Gelin, F.; Volkman, J. K.; De Leeuw, J. W.; Damsté, J. S. S., Mid-chain hydroxy long-chain fatty acids in microalgae from the genus Nannochloropsis. *Phytochemistry* **1997,** *45*, (4), 641-646.
33. Xu, Y.; Simoneit, B. R.; Jaffé, R., Occurrence of long-chain n-alkenols, diols, keto-ols and sec-alkanols in a sediment core from a hypereutrophic, freshwater lake. *Organic Geochemistry* **2007,** *38*, (6), 870-883.
34. Kim, M.; Jung, J.-h.; Jin, Y.; Han, G. M.; Lee, T.; Hong, S. H.; Yim, U. H.; Shim, W. J.; Choi, D.-L.; Kannan, N., Origins of suspended particulate matter based on sterol distribution in low salinity water mass observed in the offshore East China Sea. *Marine Pollution Bulletin* **2016,** *108*, (1), 281-288.
35. Oldenburg, T. B. P.; Jones, M.; Huang, H.; Bennett, B.; Shafiee, N. S.; Head, I.; Larter, S. R., The controls on the composition of biodegraded oils in the deep subsurface – Part 4. Destruction and production of high molecular weight non-hydrocarbon species and destruction of aromatic hydrocarbons during progressive in-reservoir biodegradation. *Organic Geochemistry* **2017,** *114*, 57-80.
36. Barros, E. V.; Dias, H. P.; Pinto, F. E.; Gomes, A. O.; Moura, R. R.; Neto, A. C.; Freitas, J. C.; Aquije, G. M.; Vaz, B. G.; Romão, W., Characterization of naphthenic acids in thermally degraded petroleum by ESI (−)-FT-ICR MS and 1H NMR after solid-phase extraction and liquid/liquid extraction. *Energy & Fuels* **2018,** *32*, (3), 2878-2888.
37. Terra, L. A.; Filgueiras, P. R.; Tose, L. V.; Romao, W.; de Souza, D. D.; de Castro, E. V.; de Oliveira, M. S.; Dias, J. C.; Poppi, R. J., Petroleomics by electrospray ionization FT-ICR mass spectrometry coupled to partial least squares with variable selection methods: prediction of the total acid number of crude oils. *Analyst* **2014,** *139*, (19), 4908-4916.
38. Benigni, P.; Sandoval, K.; Thompson, C. J.; Ridgeway, M. E.; Park, M. A.; Gardinali, P.; Fernandez-Lima, F., Analysis of photoirradiated water accommodated fractions of crude oils using tandem TIMS and FT-ICR MS. *Environmental Science & Technology* **2017,** *51*, (11), 5978-5988.
39. Silva, R. C.; Yim, C.; Radović, J. R.; Brown, M.; Weerawardhena, P.; Huang, H.; Snowdon, L. R.; Oldenburg, T. B. P.; Larter, S. R., Mechanistic insights into sulfur rich oil formation, relevant to geological carbon storage routes. A study using (+) APPI FTICR-MS analysis. *Organic Geochemistry* **2020,** *147*, 104067.
40. Chen, X.; Liu, X.; Lin, D.-C.; Wang, J.; Chen, L.; Yu, P.-S.; Wang, L.; Xiong, Z.; Chen, M.-T., A potential suite of climate markers of long-chain n-alkanes and alkenones preserved in the top sediments from the Pacific sector of the Southern Ocean. *Progress in Earth and Planetary Science* **2021,** *8*, (1), 23.

41. Guthrie-Nichols, E.; Grasham, A.; Kazunga, C.; Sangaiah, R.; Gold, A.; Bortiatynski, J.; Salloum, M.; Hatcher, P., The effect of aging on pyrene transformation in sediments. *Environmental Toxicology and Chemistry: An International Journal* **2003,** *22*, (1), 40-49.
42. Machala, M.; Ciganek, M.; Bláha, L.; Minksová, K.; Vondráček, J., Aryl hydrocarbon receptor-mediated and estrogenic activities of oxygenated polycyclic aromatic hydrocarbons and azaarenes originally identified in extracts of river sediments. *Environmental Toxicology and Chemistry* **2001,** *20*, (12), 2736-2743.
43. Bakar, N. A.; Tay, K. S.; Omar, N. Y. M.; Abas, M. R. B.; Simoneit, B. R., The geochemistry of aliphatic and polar organic tracers in sediments from Lake Bera, Malaysia. *Applied Geochemistry* **2011,** *26*, (8), 1433-1445.
44. Li, Y.; Lou, Y.; Mu, T.; Ke, A.; Ran, Z.; Xu, J.; Chen, J.; Zhou, C.; Yan, X.; Xu, Q.; Tan, Y., Sphingolipids in marine microalgae: Development and application of a mass spectrometric method for global structural characterization of ceramides and glycosphingolipids in three major phyla. *Analytica Chimica Acta* **2017,** *986*, 82-94.
45. Lipid Maps Sphingolipids [SP] (W) --> Ceramides [SP02]. https://www.lipidmaps.org/data/structure/LMSDSearch.php?Mode=ProcessClassSearch&LMID=LMSP02
46. Cheung, Y. Y.; Cheung, S.; Mak, J.; Liu, K.; Xia, X.; Zhang, X.; Yung, Y.; Liu, H., Distinct interaction effects of warming and anthropogenic input on diatoms and dinoflagellates in an urbanized estuarine ecosystem. *Global Change Biology* **2021,** *27*, (15), 3463-3473.
47. Metcalf, J. S.; Banack, S. A.; Wessel, R. A.; Lester, M.; Pim, J. G.; Cassani, J. R.; Cox, P. A., Toxin Analysis of Freshwater Cyanobacterial and Marine Harmful Algal Blooms on the West Coast of Florida and Implications for Estuarine Environments. *Neurotoxicity Research* **2021,** *39*, (1), 27-35.
48. Walker, J. S.; Keely, B. J., Distribution and significance of chlorophyll derivatives and oxidation products during the spring phytoplankton bloom in the Celtic Sea April 2002. *Organic Geochemistry* **2004,** *35*, (11-12), 1289-1298.
49. Nelson, R. K.; Gosselin, K. M.; Hollander, D. J.; Murawski, S. A.; Gracia, A.; Reddy, C. M.; Radović, J. R., Exploring the Complexity of Two Iconic Crude Oil Spills in the Gulf of Mexico (Ixtoc I and Deepwater Horizon) Using Comprehensive Two-Dimensional Gas Chromatography (GC × GC). *Energy & Fuels* **2019,** *33*, (5), 3925-3933.
50. Bixian, M.; Jiamo, F.; Gan, Z.; Zheng, L.; Yushun, M.; Guoying, S.; Xingmin, W., Polycyclic aromatic hydrocarbons in sediments from the Pearl river and estuary, China: spatial and temporal distribution and sources. *Applied Geochemistry* **2001,** *16*, (11), 1429-1445.
51. Niu, L.; Yang, Q.; van Gelder, P.; Zeng, D.; Cai, H.; Liu, F.; Luo, X., Field analysis of PAHs in surface sediments of the Pearl River Estuary and their environmental impacts. *Environmental Science and Pollution Research* **2020,** *27*, (10), 10925-10938.
52. Ni, H.-G.; Lu, F.-H.; Luo, X.-L.; Tian, H.-Y.; Zeng, E. Y., Occurrence, Phase Distribution, and Mass Loadings of Benzothiazoles in Riverine Runoff of the Pearl River Delta, China. *Environmental Science & Technology* **2008,** *42*, (6), 1892-1897.
53. Wang, J.-Z.; Nie, Y.-F.; Luo, X.-L.; Zeng, E. Y., Occurrence and phase distribution of polycyclic aromatic hydrocarbons in riverine runoff of the Pearl River Delta, China. *Marine Pollution Bulletin* **2008,** *57*, (6), 767-774.
54. Vairavamurthy, A.; Mopper, K., Geochemical formation of organosulphur compounds (thiols) by addition of H2S to sedimentary organic matter. *Nature* **1987,** *329*, (6140), 623-625.
55. Zhu, M.; Jiang, B.; Li, S.; Yu, Q.; Yu, X.; Zhang, Y.; Bi, X.; Yu, J.; George, C.; Yu, Z.; Wang, X., Organosulfur Compounds Formed from Heterogeneous Reaction between SO2 and Particulate-Bound Unsaturated Fatty Acids in Ambient Air. *Environmental Science & Technology Letters* **2019,** *6*, (6), 318-322.

56. Damste, J. S. S.; De Leeuw, J. W., Analysis, structure and geochemical significance of organically-bound sulphur in the geosphere: state of the art and future research. *Organic Geochemistry* **1990,** *16*, (4-6), 1077-1101.